Joint International Topical Meeting on Mathematics & Computation and Supercomputing in Nuclear Applications (M&C + SNA 2007)
Monterey, California, April 15-19, 2007, on CD-ROM, American Nuclear Society, LaGrange Park, IL (2007)

FLUX-LIMITED DIFFUSION COEFFICIENTS IN REACTOR PHYSICS APPLICATIONS

Justin Pounders and Farzad Rahnema
Nuclear and Radiological Engineering / Medical Physics Program
George W. Woodruff School of Mechanical Engineering
Georgia Institute of Technology
Atlanta, GA 30332-0405
farzad.rahnema@nre.gatech.edu

Ronaldo Szilard
Idaho National Laboratory/Nuclear Programs
Nuclear Science and Engineering Division
Idaho Falls, ID 83415

ABSTRACT

Flux-limited diffusion theory has been successfully applied to problems in radiative transfer and radiation hydrodynamics, but its relevance to reactor physics has not yet been explored. The current investigation compares the performance of a flux-limited diffusion coefficient against the traditionally defined transport cross section. A one-dimensional BWR benchmark problem is examined at both the assembly and full-core level with varying degrees of heterogeneity.

Key Words: Flux-limited Diffusion Theory; Monte Carlo Methods; Reactor Analysis; Transport Cross Section; Diffusion Coefficient

1. INTRODUCTION

Diffusion theory is perhaps the most common approximation of the transport equation for large-scale reactor problems. The accuracy of diffusion methods, particularly in fine mesh problems, depends on the choice of diffusion coefficient. Traditional diffusion methods have used the first angular moment of the transport equation (the P_1 equation) to close the angle-integrated transport equation by forming an expression of Fick's Law. The intermediate approximations involved in this process, however, often break down in the presence of strong neutron absorbers or steep flux gradients, limiting its applicability to practical nuclear engineering problems.

Levermore and Pomraning [1] proposed a flux-limited diffusion theory to alleviate some of these inaccuracies for radiative transfer problems. Specifically, the flux-limited diffusion theory they proposed eliminates causality violations—unphysical conditions in which, using neutronic terminology, the particle current exceeds the scalar flux. Flux-limited diffusion theory has been successfully applied to problems in the fields of radiative transfer and radiation hydrodynamics [2, 3], but its relevance to reactor physics has not yet been determined.

As a preliminary investigation, therefore, a P_1-based flux-limited diffusion coefficient derived by Pomraning [6] is compared with the 'classical' definition for a series of one-dimensional

problems with varying scale and heterogeneity. The next section will discuss the classical and flux-limited diffusion coefficients and the approximations associated with both, followed by some numerical results.

2. DIFFUSION COEFFICIENTS

2.1. Classical diffusion coefficient

Classical diffusion theory is based on the P_1 approximation to the transport equation. The time-independent multigroup formulation of these equations can be written [4]

$$\nabla \cdot \mathbf{J}_g(\mathbf{r}) + \sigma_g(\mathbf{r})\varphi_g(\mathbf{r}) = S_{0,g}(\mathbf{r}) + \sum_{g'=1}^{G} \sigma_{s,0}^{g'g}(\mathbf{r})\varphi_{g'}(\mathbf{r}) \tag{1}$$

$$\nabla \varphi_g(\mathbf{r}) + 3\sigma_g(\mathbf{r})\mathbf{J}_g(\mathbf{r}) = 3\sum_{g'=1}^{G} \sigma_{s,1}^{g'g}(\mathbf{r})\mathbf{J}_{g'}(\mathbf{r}) . \tag{2}$$

where $\mathbf{J}(\mathbf{r}) = \int_{4\pi} \hat{\Omega}\psi(\mathbf{r},\hat{\Omega})$ is the neutron current. The only approximation made in these equations is that the angular flux is linearly anisotropic.

Traditionally, Equation (2) has been recast in a form similar to Fick's Law by the additional approximation

$$\sum_{g'=1}^{G} \sigma_{s,1}^{g'g}(\mathbf{r})\mathbf{J}_{g'}(\mathbf{r}) = \sum_{g'=1}^{G} \sigma_{s,1}^{gg'}(\mathbf{r})\mathbf{J}_g(\mathbf{r}) . \tag{3}$$

This equation is a form of detailed balance which is a good approximation in the presence of heavy scattering. Using this expression in Equation (2) results in

$$\nabla \varphi_g(\mathbf{r}) = -3\left[\sigma_g(\mathbf{r}) - \sum_{g'=1}^{G} \sigma_{s,1}^{gg'}(\mathbf{r})\right]\mathbf{J}_g(\mathbf{r}) \tag{4}$$

The term in brackets is typically defined as the transport cross section, $\sigma_{tr,g}$. This definition of the transport cross section is referred to as the 'classical' definition and denoted by a *C* superscript:

$$\sigma_{tr,g}^{C}(\mathbf{r}) = \sigma_g(\mathbf{r}) - \sum_{g'=1}^{G} \sigma_{s,1}^{gg'}(\mathbf{r}) . \tag{5}$$

By letting $\sigma_{s,\ell}^{g} = \sum_{g'=1}^{G} \sigma_{s,\ell}^{gg'}(\mathbf{r})$ and defining the average scattering angle as $\bar{\mu}_{0,g} = \dfrac{\int_{-1}^{1} \mu_0 \sigma_s^g(\mu_0) d\mu_0}{\int_{-1}^{1} \sigma_s^g(\mu_0) d\mu_0}$,

Equation (5) can be cast into a more common form:

$$\sigma_{tr,g}^{C}(\mathbf{r}) = \sigma_g(\mathbf{r}) - \bar{\mu}_{0,g}\sigma_{s,0}^{g} \tag{6}$$

Equation (4) is now in the form of Fick's law, $\mathbf{J} = -D\nabla\varphi$, implying the following definition of the diffusion coefficient:

$$D_g^C = -\frac{1}{3\sigma_{tr,g}^{C}} . \tag{7}$$

2.2. Flux-limited diffusion coefficient

Through his investigation of flux-limited diffusion theory, Pomraning [6] derived a new formulation of the transport cross section which may improve upon classical diffusion results. The essence of his formulation is the assumption that the angular flux can be decomposed into a scalar component and normalized angular factor, and furthermore, the normalized angular factor is independent of the energy group. Quantitatively,

$$\psi_g(\mathbf{r},\hat{\Omega}) = \varphi_g(\mathbf{r})\Psi(\mathbf{r},\hat{\Omega}) \tag{8}$$

where $\int_{4\pi} d\hat{\Omega}\Psi(\mathbf{r},\hat{\Omega}) = 1$. Multiplying this equation by $\hat{\Omega}$ and integrating over all directions, then taking the ratio of two different groups implies that

$$\frac{\mathbf{J}_g(\mathbf{r})}{\varphi_g(\mathbf{r})} = \frac{\mathbf{J}_{g'}(\mathbf{r})}{\varphi_{g'}(\mathbf{r})}. \tag{9}$$

Upon plugging this separation into the second P_1 equation [Equation (2)], the following definition of the transport cross section arises, which will be denoted by the superscript *FL*:

$$\sigma_{tr,g}^{FL}(\mathbf{r}) = \sigma_g(\mathbf{r}) - \sum_{g'=1}^{G} \frac{\sigma_{s,1}^{g'g}(\mathbf{r})\varphi_{g'}(\mathbf{r})}{\varphi_g(\mathbf{r})}. \tag{10}$$

This definition of the transport cross section avoids the detailed balance approximation of Equation (3), but makes the additional assumption that the angle and energy dependencies of the flux can be separated.

Equation (10) can also be derived as a limiting case of the more general flux-limited diffusion theory presented by Levermore and Pomraning [1] in which Fick's law is written

$$\mathbf{J}_g = -\left[\frac{\lambda_g(R_g)}{\sigma_g\omega_g}\right]\nabla\varphi_g. \tag{11}$$

The parameter, λ_g, is a function of the dimensionless spatial flux gradient, $R_g = \left(\sigma_g\omega_g\varphi_g\right)^{-1}\left|\nabla\varphi_g\right|$, and ω_g is the effective mean number of secondary neutrons per collision. The complete derivation is quite lengthy and will not be repeated here, but Pomraning showed that in the limit of a weak spatial variations of the flux (i.e. $R_g \to 0$ and $\nabla\cdot\mathbf{J}_g = 0$), Equation (11) can be written

$$\mathbf{J}_g = -\frac{1}{3}\left[\sigma_g - \sigma_g(\mathbf{r}) - \sum_{g'=1}^{G}\frac{\sigma_{s,1}^{g'g}(\mathbf{r})\varphi_{g'}(\mathbf{r})}{\varphi_g(\mathbf{r})}\right]\nabla\varphi_g \tag{12}$$

which leads exactly to the definition of the transport cross section shown by Equation (10).

2.3. Implementation

The Monte Carlo code MCNP5 [7] was modified to calculate the classical and flux-limited transport cross sections defined above. Specifically, MCNP was modified to tally the total cross

section and the first Legendre moment of the group-to-group scattering matrix for arbitrary group structures and sub-regions of the system [10]. With these cross sections and the group averaged flux, the transport cross sections defined by Equations (5) and (10) can be calculated.

3. RESULTS

The one-dimensional BWR benchmark problem described in Appendix A, was examined using both the classical and flux-limited diffusion theories described in the previous section. The benchmark was analyzed at both the fuel assembly and full-core levels.

The modified version of MCNP5 was used to generate 2-group benchmark solutions and calculate material-wise classical and flux-limited diffusion coefficients for each material region in the assembly and full-core problems. The diffusion code NESTLE [9] was then used to generate a fine-mesh, finite-difference 2-group diffusion solution for each benchmark case using both the classical and flux-limited diffusion coefficients. Since both the transport and diffusion calculations are based on the same 2-group library, the resulting errors should reflect only the performance of the diffusion coefficients.

3.1. Assembly-level results

Table I shows the eigenvalue differences between the transport and diffusion solutions for the four types of fuel assemblies with specular reflection on the boundaries. Table I also shows the average fast and thermal flux errors. It is seen that, in general the flux-limited diffusion coefficient produces less accurate eigenvalues and flux distribution solutions. Figures 1 and 2 display the values of the transport cross section for assembly 1 (the most homogenous) and assembly 3 (the most heterogeneous).

The average statistical relative error in the fast diffusion coefficient is 0.2%, while the average thermal relative error is 0.06%. In all cases, the flux-limited cross section is statistically distinct from the classical transport cross section, having absolute differences greater than three standard deviations.

Table I. Assembly Level Errors

		Δk_{eff}* [mk]		Avg Flux Errors (fast / thermal)	
Assembly	$k_{eff} \pm 0.03$ mk	Classical	Flux-limited	Classical	Flux-limited
1	1.18099	1.24	1.97	0.29% / 0.31%	1.00% / 0.75%
2	1.23736	1.17	2.07	1.13% / 0.61%	1.05% / 0.62%
3	0.61445	-6.14	-9.89	1.56% / 1.82%	1.61% / 2.81%
4	0.31073	-0.56	-0.52	1.06% / 3.11%	0.96% / 4.16%

*$\Delta k_{eff} = [k_{\text{DIFFUSION}} - k_{\text{MCNP}}]$*1000 mk

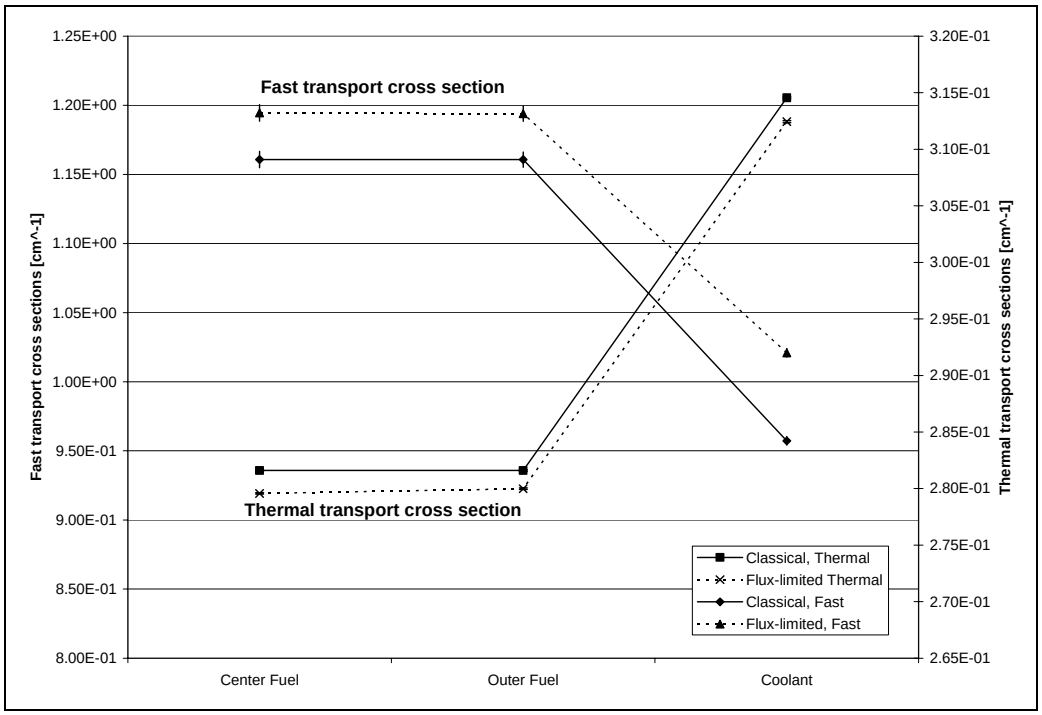

*Error bars corresponding to statistical uncertainty are included above, but may not be visible due to the small values

Figure 1. Assembly 1 Transport Cross Sections

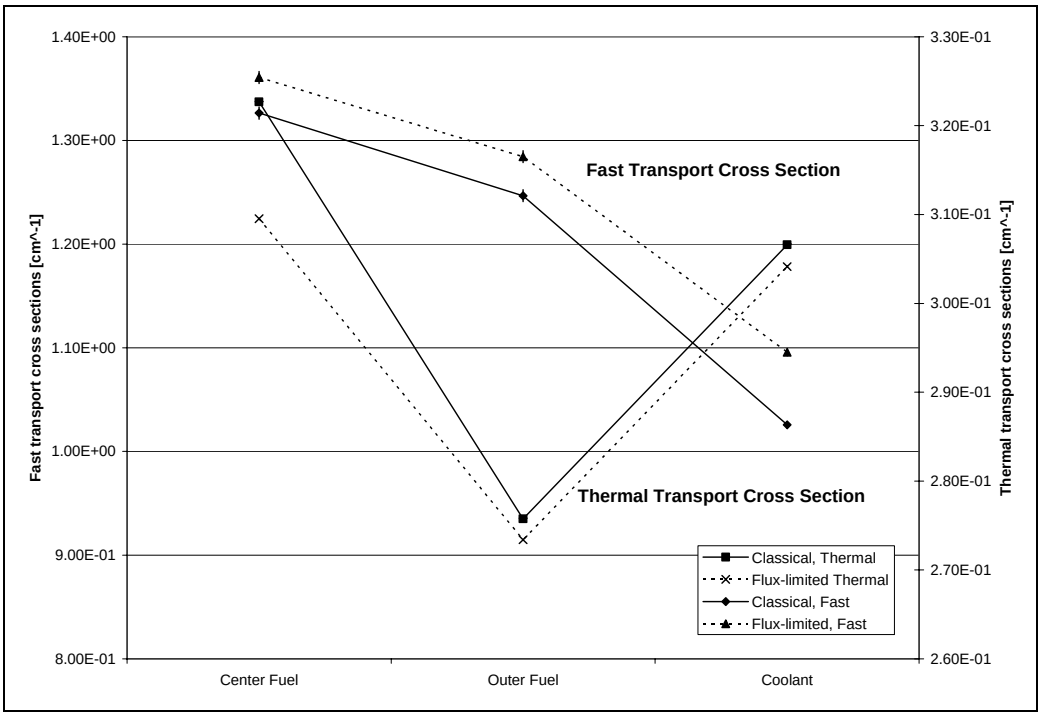

*Error bars corresponding to statistical uncertainty are included above, but may not be visible due to the small values

Figure 2. Assembly 3 Transport Cross Sections

3.2. Full-core results

Table II shows the diffusion eigenvalue errors associated with the three whole core configurations. Again it is seen that the flux-limited transport cross section produces slightly less accurate eigenvalue estimates. Figures 3-5 show the assembly averaged flux errors for the three core configurations (only the first four of seven assemblies are shown since there is symmetry about the center). It is seen that the flux-limited results are consistently poorer in the thermal group, but perform slightly better in the fast group in approximately half of the regions, particularly away from the boundaries.

Table II. Core Eigenvalue Differences

		Δk_{eff}^{*} [mk]	
Configuration	$k_{eff} \pm 0.03$ mk	Classical	Flux-limited
1	1.16818	0.92	1.22
2	0.94224	-3.47	-3.55
3	0.78916	-6.53	-7.04

*$\Delta k_{eff} = [k_{\text{DIFFUSION}} - k_{\text{MCNP}}]$*1000 mk

To understand these errors, it is insightful to consider the approximations that were necessary in deriving each of the diffusion coefficients. The primary assumption made in deriving the classical diffusion coefficient was Equation (4), which presumed a scattering dominant medium. The primary assumption made in deriving the flux-limited diffusion coefficient was the legitimacy of operating in the limit of weak spatial variation.

The first assumption of scattering dominance is well supported. In fact, the scattering to total cross sections ratio ($\sigma_{s,g} / \sigma_g$) is greater than 0.9 in all regions except those containing gadolinium, where the ratio drops to around 0.6 in the thermal group.

The second assumption of weak spatial variation is not as easily justified, however. The dimensionless gradient parameter, $R_g = \left(\sigma_g \omega_g \varphi_g\right)^{-1} \left|\nabla \varphi_g\right|$, was estimated for all regions of the problem. The mean value of *R* was 0.3 in the fast group and 0.4 in the thermal group, but peaked considerably near the vacuum boundaries of the cores, and at material interfaces where the material properties changed sharply, reaching maximum values of 1.4 and 2.7 in the fast and thermal groups, respectively. This explains the observation that the flux-limited diffusion coefficient performs better in the fast group, where the gradients are less severe, but deteriorates near boundaries and as the level of heterogeneity increases.

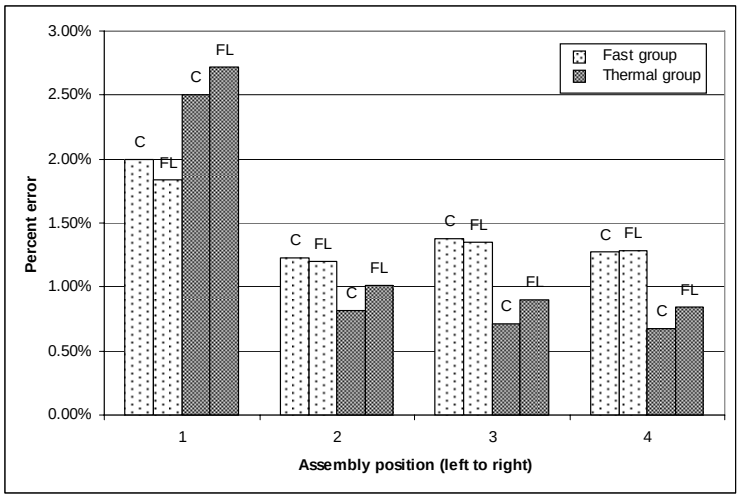

Figure 3. Average Flux Errors in Core 1

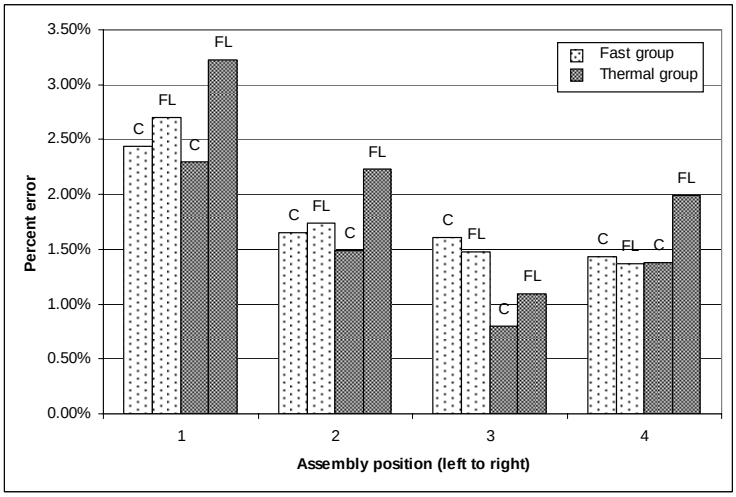

Figure 4. Average Flux Errors in Core 2

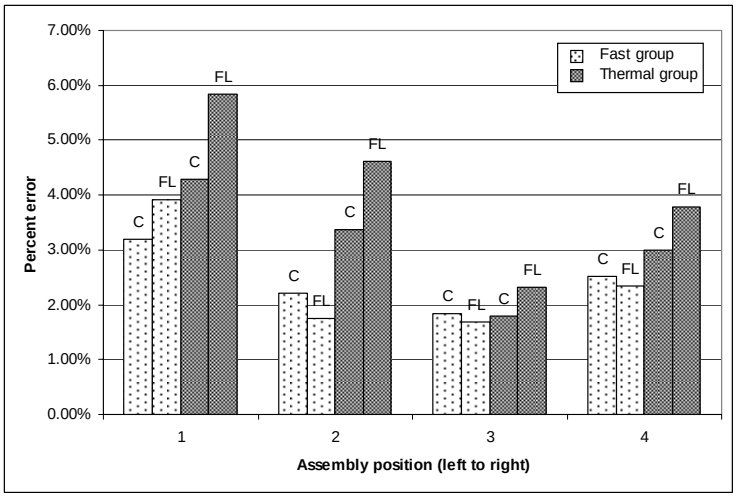

Figure 5. Average Flux Errors in Core 3

4. CONCLUSIONS

These results signify that the present definition of the flux-limited diffusion coefficient does not perform better than the traditional definition of the transport cross section. This can be attributed to the presence of significant spatial variations which violate the assumption made in deriving this particular definition. Even in core configuration 1, which is quite smooth spatially, the current definition performs, at best, comparably with the traditional definition.

Future work should investigate more advanced flux-limiting diffusion coefficients which account for arbitrary spatial gradients, i.e. compute D as a function of R instead of in the limit of small R [see Eq. (11)]. This of course introduces nonlinearities into the diffusion equation, a problem that was addressed in the context of radiative transfer by Szilard and Pomraning [11]. Preliminary investigations have shown that this more general flux-limited diffusion coefficient does indeed produce more accurate results for reactor problems than traditional diffusion theory [12]. In these investigations, the diffusion coefficients were generated *a priori* by a deterministic transport method. This becomes problematic for stochastic transport methods, however, since there is not a practical method for generating local spatial flux gradients. The present authors are currently exploring this and related issues regarding Monte Carlo-based diffusion coefficient calculations which they hope to discuss in the near future.

ACKNOWLEDGMENTS

The first author performed this work under appointment to the Naval Nuclear Propulsion Fellowship Program sponsored by Naval Reactors Division of the U.S. Department of Energy.

REFERENCES

1. Levermore, C. D. and Pomraning, G. C., "A flux-limited diffusion theory," *The Astrophysical Journal*, **248**, 321 (1981).
2. Olson, G. L., Auer, L. H. and Hall, M. L., "Diffusion, P1, and other approximate forms of radiation transport," *Journal of Quantitative Spectroscopy and Radiative Transfer*, **64**, 619 (2000).
3. Turner, N. J. and Stone, J. M., "A Module for Radiation Hydrodynamic Calculations with ZEUS-2D Using Flux-limited Diffusion," *The Astrophysical Journal Supplement Series*, **135**, 95 (2001).
4. Bell, G. and Glasstone, S. *Nuclear Reactor Theory*, Robert E. Krieger Publishing Co., Huntington, NY (1979).
5. Stamm'ler, R. J. J., *Methods of Steady-State Reactor Physics in Nuclear Design*, Academic Press Inc., London (1983).
6. Pomraning, G. C., "Flux-Limited Diffusion Theory with Anisotropic Scattering," *Nuclear Science and Engineering*, **86**, 335 (1984).
7. Brown, F. et al, "MCNP Version 5," *Transactions of the American Nuclear Society*, **87**, 273 (2003).
8. D. Ilas, F. Rahnema, "A Heterogeneous Coarse Mesh Transport Method," *Transport Theory and Statistical Physic*, **32** (5-7), 445-471, 2003.

9. Turinsky, F. et al, “NESTLE: A Few Group Neutron Diffusion Equation Solver Utilizing the Nodal Expansion Method (NEM) for Eigenvalue, Adjoint, and Fixed-Source Steady-State and Transient Problems,” EGG-NRE-11406 (1994).
10. Pounders, J., Rahnema, F. and Stamm’ler, R. J. J. “Title,” PHYTRA
11. Szilard, R. H. and Pomraning, G. C. “Numerical Transport and Diffusion Methods in Radiative Transfer.” *Nuclear Science and Engineering*, **112**, 256 (1992).
12. Keller, S. and Rahnema, F. Private communication (2007).

Appendix A

The geometry of the one-dimensional BWR core was taken from Ilas D. and Rahnema (2003). Figure A.I shows the core composition and geometry. Each material region is homogeneous and uniform. Table A.I summarizes the dimensions of the core

The ‘water’ is actually a coolant and zirconium mixture. Fuel I and fuel II are 2.2% and 3.6% enriched UO_2, respectively, mixed with light water and zirconium. Fuel + Gd is a fuel, zirconium and water mixture with 4.0% enriched uranium and 4% gadolinium. Vacuum boundary conditions were assigned to the left and right boundaries.

Each core can be divided into seven fuel assemblies. An assembly consists of four contiguous fuel regions with a region of water on either side. Each core therefore contains two unique assembly types which appear in an alternating pattern.

Table A.I. Core Dimensions

Water slab width	1.1176 cm
Fuel slab width	3.2512 cm
Total core width	106.68 cm

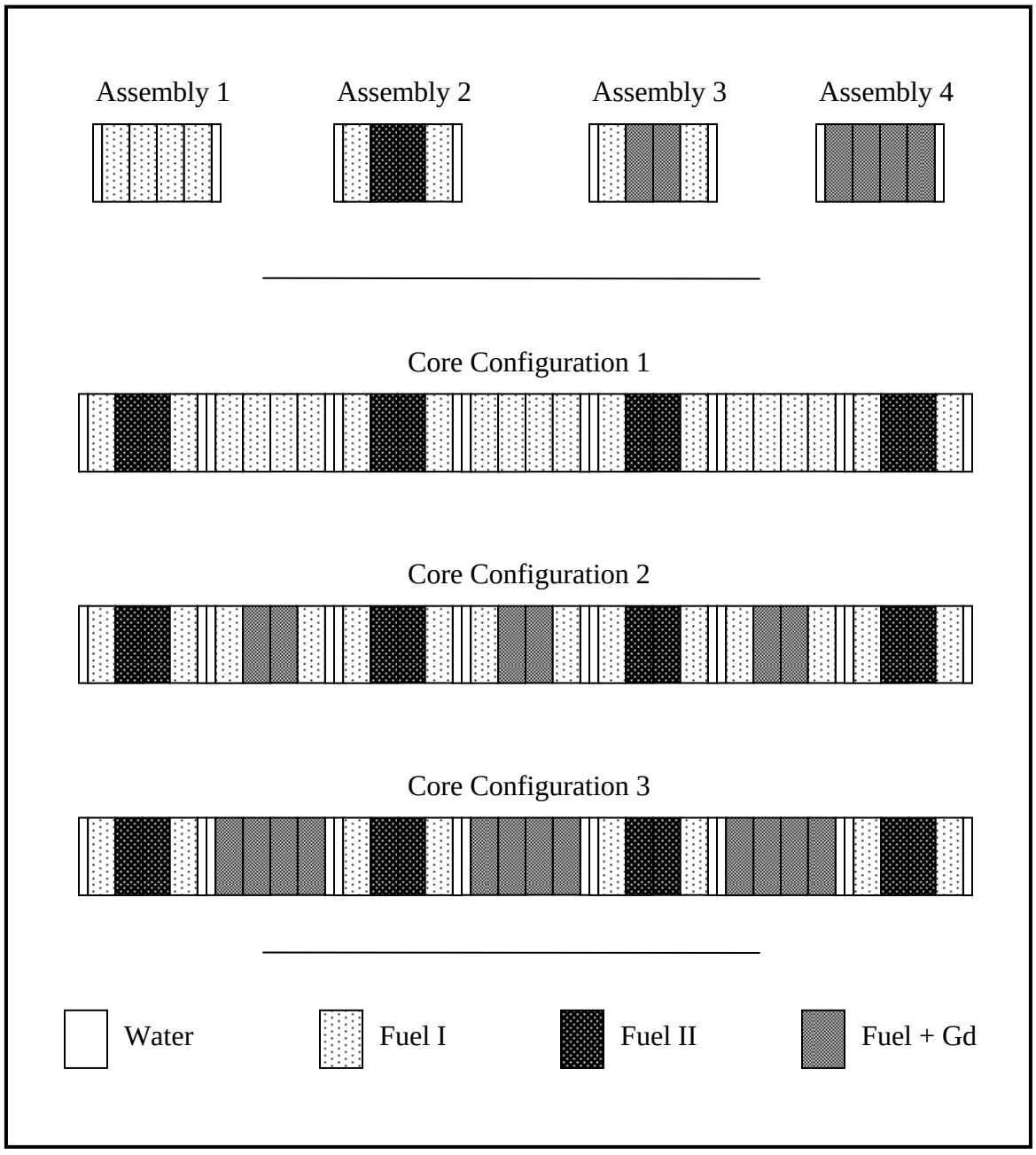

Figure A.1. Assembly and Core Composition and Geometry